In Situ Techniques for the Characterization of Alkaline Urea Oxidation Reaction

Xu Yang [1], Huimin Zhang [2], Binbin Yu [3], Yan Liu [4], Zucheng Wu [1*]

1 Department of Environmental Engineering, Zhejiang University, Hangzhou 310058, China
2 Department of Environmental Engineering, East China Jiaotong University, Nanchang 330013, China
3 College of Pharmaceutical and Chemical Engineering, Taizhou University, Taizhou 318000, Zhejiang, China
4 School of Earth Sciences, Zhejiang University, Hangzhou 310058, China
*Corresponding Author: wuzc@zju.edu.cn

ABSTRACT

Developing high-efficiency and affordable electro-catalysts remains a crucial bottleneck on the way to the practical applications of the electrochemical urea oxidation reaction (UOR) scenarios. In recent years, Ni-based materials have proven to be excellent electrocatalysts for the UOR in alkaline medium. Understanding the characteristics that affect UOR activity and determining the mechanism are of vital importance for the development of UOR electro-catalysts. Therefore, in situ characterization techniques performed under UOR conditions are urgently needed to monitor the key intermediates together with identifying the UOR active centers and phases. Herein, recent advances regarding in situ techniques for the characterization of Ni-based electrocatalysts are summarized, including Raman spectroscopy, X-ray diffraction, Fourier transform infrared spectroscopy. The results from these in situ measurements not only reveal the structural transformation of the catalytic species under UOR conditions, but also disclose the crucial role of NiOOH during the UOR. The evidence displayed by identified intermediate product information helps scientists better understand the UOR path and find solutions. Furthermore, those knowledge will provide helpful inspiration and guidance for the further development of high-efficiency UOR catalysts.

Keywords: in situ techniques, urea oxidation reaction, active phases, reaction species

1. INTRODUCTION

The increasing demands in energy and awareness of negative environmental impact have accelerated the transition from fossil fuels to green alternative energies (such as solar, wind, and tidal energy). However, these renewable energies are unpredictable due to the daily, seasonal, and regional factors, limiting their widespread adoption in the global energy mix. [1, 2] Thus, it is imperative to develop innovative energy conversion and storage technologies. Urea is a highly potential energy / hydrogen carrier among various sustainable energy carrier candidates. [3-5] The electrochemical approach is a vital way to transform the chemical energy in urea. The urea oxidation reaction (UOR; $CO(NH_2)_2 + 6OH^- = N_2 + CO_2 + 5H_2O + 6e^-$) is a crucial half reaction in the fields of urea fuel cells, urea-assisted hydrogen production, etc. [6-11]

For the sluggish $6e^-$ transfer process, the exploitation of high-efficiency electrocatalysts is urgently needed to speed up the UOR and reduce the overpotential to minimize the energy loss inherent in the energy conversion technologies. Extensive efforts have been devoted to develop earth-abundant and high-performance electrocatalysts for UOR, and Ni-based materials have proven to be excellent. [5, 11-13]

For electrooxidation reactions on Ni-based species, the $Ni(OH)_2/NiOOH$ redox pair, i.e. Ni(II)/Ni(III) couple, is often considered to have a significant effect, and it is the Ni(III) species that initiate the oxidation reaction. [14, 15] This understanding has been widely accepted in the research of UOR catalysts. [16-22] Cyclic voltammetry (CV), linear sweep voltammetry (LSV), and

rotating disc electrode (RDE) voltammetry are frequently used to investigate the electrocatalytic behavior of urea oxidation on a nickel electrode in alkaline medium. [16] The UOR occurs after the formation of some amount of Ni(III) on the electrode surface. The observed decrease in cathodic charge when urea is present in KOH solution suggests a possible indirect oxidation (catalyst regeneration-EC') mechanism (Eqs. (1)–(3)). Nevertheless, this decrease can be attributed to another possibility. Our group's work [10, 13, 17] about the UOR on Ni/CNT@Sponge, NiCo/C bimetallic nanoparticles, NiM double hydroxides (M = Cr, Mn, Fe, Co, Cu, Zn) catalysts obtained sufficient electrochemical characterization results, which supported this indirect oxidation process and suggested that high-valence Ni species play an important role in UOR. Also, Guo et al. [23] used electrochemical impedance spectroscopy (EIS) to systematically analyze UOR in alkaline medium. Their results show both indirect and direct pathways proceed in urea electrooxidation process.

EC' mechanism:

E $6Ni(OH)_{2(s)} + 6OH^- \leftrightarrow 6NiOOH_{(s)} + 6H_2O_{(l)} + 6e^-$ (1)

C $6NiOOH_{(s)} + CO(NH_2)_{2(aq)} + H_2O_{(l)} \rightarrow 6Ni(OH)_{2(s)} + N_{2(g)} + CO_{2(g)}$ (2)

Net anodic reaction:

EC' $CO(NH_2)_{2(aq)} + 6OH^- \rightarrow N_{2(g)} + 5H_2O_{(l)} + CO_{2(g)} + 6e^-$ (3)
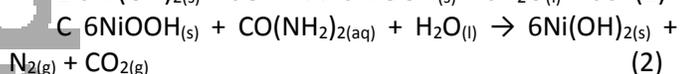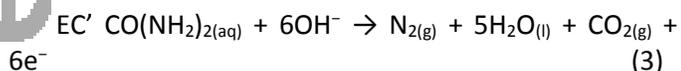
On the one hand, in view of classical electrochemical methods usually provide indirect and incomplete information about the reaction kinetics, thus it is difficult to correctly elucidate the mechanism of UOR. Therefore, obtaining direct evidence on the electrocatalyst species evolution or reaction species identification under the actual conditions of electrooxidation reactions is undoubtedly more convincing for the study of the UOR mechanism. Recently, some advanced methods, such as Raman spectroscopy, X-ray diffraction (XRD), Fourier transform infrared spectroscopy (FTIR), are used to in situ monitor the UOR process to detect the actual active phases and the electrochemical behavior during UOR on the surface of the electrocatalyst. On the other hand, there were some meaningful reviews on the UOR, including the relevant nickel-based electrocatalysts and UOR-based energy conversion technologies, such as urea electrolysis, photoelectrochemical urea splitting, and urea fuel cells. The development and improvement of electrocatalysts and the application evaluation of UOR-based energy technologies are important and indispensable. Furthermore, an in-depth understanding of the working mechanism of high-efficiency UOR catalysts and intermediate products of urea oxidation can provide clues and guidance for catalyst design and development.

As mentioned earlier, in situ observation methods can play a key role in this field. However, to our best knowledge, there is a lack of systematic attention to the progress of UOR-related in situ monitoring work. A typical overview and summary of these in situ characterization results is therefore highly needed. Herein, we summarize the applications of in situ techniques in the investigation of the UOR mechanism, to show the significant role of high-valence Ni species (Ni[III]) in the UOR and the recognition of important intermediates.

2. IN SITU TECHNIQUES

2.1 In situ Raman and surface-enhanced Raman spectroscopy

Raman spectroscopy is a vibrational spectroscopic technique that observes vibration, rotational, and other low-frequency modes. [24] Therefore, it is a powerful tool in the chemical and materials sciences owing to its high molecular specificity, high sensitivity in the low frequency range (where M−OH, M−OH₂, and M=O vibrations appear), and noninterference of water. In view of all these strengths, Raman spectroscopy is particularly applicable to in situ monitoring of the intermediates during the electrochemical systems performed in aqueous media. [25] A combination of Raman spectroscopy and electrochemistry can provide real-time spectroscopic information that helps to understand how an electrochemically driven reaction occurs. To enhance the sensitivity and spatial resolution of the Raman scattering of species on the surface, surface enhanced Raman spectroscopy (SERS) is often adopted.

Vedharathinam and Botte [26] investigated the UOR mechanism on a $Ni(OH)_2$ catalyst in alkaline medium by in situ SERS. The potential dependent SER spectra recorded in 5 M KOH indicates a pair of broad overlapping bands between 200 and 600 cm^{-1} at potentials below 0.34 V vs. Hg/HgO. Above 0.3 V vs. Hg/HgO, the broad peaks emerge into two strong peaks at 479 and 559 cm^{-1} implying the presence of Ni−O bending and Ni−O stretching vibrations characteristic of NiOOH, respectively. When 1 M urea was added, the

NiOOH doublet peak appears at 476 and 558 cm^{-1}. The occurrence of NiOOH doublet above 0.36 V vs. Hg/HgO implies that $Ni(OH)_2$ is oxidized in situ to NiOOH that catalyzes the UOR. In addition, a peak at 1003 cm^{-1} was noticed that corresponds to the symmetric C−N stretch of urea, and the intensity reduced with increasing the applied potential implying that urea is oxidized by the NiOOH catalyst. A peak at 1062 cm^{-1} assigned to the symmetric stretch of CO_3^{2-} was observed in the spectrum obtained at 0.5 V vs. Hg/HgO in 1 M urea + 5 M KOH solution. The presence of CO_3^{2-} suggests that one of the products of the UOR is CO_2 that was converted to CO_3^{2-} ions due to the prevailing high pH. Furthermore, Time resolved SER spectra performed on NiOOH surface were obtained at open-circuit conditions. The intensity of NiOOH peak did not change even after leaving the catalyst in 5 M KOH for 780 s indicating no chemical change of NiOOH. On the contrary, when recorded in 1 M urea + 5 M KOH, the intensity of the NiOOH doublet peak decreased after holding for 60 s and eventually the peaks disappeared after ~240 s. A new peak at 528 cm^{-1} related to α-$Ni(OH)_2$ was finally observed, strongly indicating that NiOOH had been chemically reduced to α-$Ni(OH)_2$ by urea. Consequently, the authors concluded that the UOR on $Ni(OH)_2$ in alkaline medium is mediated through the $NiOOH/Ni(OH)_2$ redox pair and follows the the indirect or catalyst regeneration (EC') mechanism. In the authors' another work [27] about potential oscillations during the UOR on Ni, the in situ time-resolved SER spectra on $Ni(OH)_2$ also showed the characteristic of NiOOH species in 5 M KOH without or with 0.33 M urea in potential oscillations condition. These results once again confirm the important role of NiOOH.

Nickel-based bimetallic catalysts have received much attention. Singh et al. [28] investigated Ni-deposited Sn dendrites (Ni/Sn dendrites) for UOR. The in situ SRES measurement indicates that urea oxidation on Ni/Sn dendrites is initiated by $Ni^{III}OOH$ species, as NiOOH characteristic peaks (479 and 559 cm^{-1}) appeared above 0.40 V vs. Ag/AgCl in 0.33 M urea + 1 M KOH electrolyte. Zhang et al. [29] employed Mo-doped Ni_2P nanoarrays supported on Ni foam (Mo-Ni_2P/NF) for the efficient urea degradation. Raman spectra acquired from Mo-Ni_2P in 1 M KOH with 0.1 M urea showed the disappearance of $Ni^{III}OOH$ peaks contrary to the spectra (481/561 cm^{-1}) in 1 M KOH. The author believed it is due to the rapid reduction of $Ni^{III}OOH$ to $Ni^{II}(OH)_2$ in urea-containing solutions.

Our group has recently employed an in situ SERS technique to study the evolution process of Ni-based bimetallic electrocatalysts under actual UOR conditions, and obtained some unreported data to show direct evidence of $Ni^{III}OOH$ species and high-valence state of the doped metal element. Based on the in situ Raman data reported recently, it can be summarized that NiOOH is the active phase during UOR and is accompanied by redox of nickel (oxy)hydroxides (II → III → II).

2.2 In situ X-ray diffraction (XRD)

XRD is a powerful technique for phase identification of crystalline materials. Combining XRD with electrochemical investigations can bring new opportunities for studying the electrochemical reaction pathways and the phase changes of electrode materials.

Wang and Botte [30] employed in situ XRD technique combined with electrochemical analysis to study urea electrolysis on nickel hydroxide catalysts. The evolution of XRD reflections of $Ni(OH)_2$ electrode at different cell voltages in 5 M KOH in the absence and presence of 1 M urea was obtained. In 5 M KOH at cell voltages between 1.2 V to 1.6 V, the intensities of the (100), (101), (102), (110), (111) diffraction peaks of $Ni(OH)_2$ decreased with increasing the cell voltage. Concomitantly, a new diffraction peak at ~12.7° indexed to NiOOH (003) reflection was generated and its intensity increased with increasing the cell voltage. When urea was present in the KOH solution, the XRD patterns showed that the intensities of all the diffraction peaks of $Ni(OH)_2$ are stable at the same level and no new phase (e.g., NiOOH) is formed. Combined with the electrochemical analysis that indicates $Ni(OH)_2$ catalyzes the UOR in alkaline solution, the authors concluded that both the electrochemical oxidation of $Ni(OH)_2$ and chemical reduction NiOOH occur during the whole process, and the lifetime of NiOOH is short due to its chemical reduction by urea and not detectable on the timescale of the XRD scans taking place and thus keeps the XRD patterns without any change.

Therefore, in situ XRD method can show the structural changes of catalysts during UOR in alkaline medium, and urea electrooxidation on a $Ni(OH)_2$ anode undergoes the indirect process.

2.3 In situ Fourier transform infrared spectroscopy (FTIR)

In situ FTIR is a potent tool for monitoring the key reaction species and intermediates during the reaction

[31], since IR spectra can give some idea about the type of coordination of adsorbed molecules.

Wang et al. [32] evaluated Ni-WC/C (tungsten carbide modified nickel) catalyst for the electrooxidation of urea in alkaline electrolyte and used in situ FTIR to gain insight into the synergistic effect between nickel and tungsten carbide. For the Ni/C catalyst, the absorbance spectra showed several peaks above 0.4 V vs. Hg/HgO. The most prominent negative-going band around 1640 cm^{-1} is assigned to the OH bending mode representing the change in OH$^-$ concentration near the electrode during the formation of NiOOH. Another negative-going peak seen at 1470 cm^{-1}, represents cleavage of the C–N bonds. For Ni-WC/C, both negative bands appeared at 0.40 V, which is ~50 mV lower than those on Ni/C. This implies that the C–N bond can be more easily broken on Ni-WC/C surfaces, thus leading to a lower overpotential of UOR. Additionally, the formation of CO_3^{2-} and HCO_3^- were confirmed by the positive-going peaks at 1380 cm^{-1} and 1234 cm^{-1}, respectively, due to the CO_2 produced during the urea oxidation. For the assignment of the positive band at 2168 cm^{-1}, in situ FTIR study was conducted on Ni/C during the CO stripping measurement. The results showed no bands were observed between 2200 and 1900 cm^{-1}, indicating that the 2168 cm^{-1} band is not related to adsorbed CO. IR spectrum was further collected at 0.7 V vs. Hg/HgO during the UOR on Ni/C under s-polarized IR radiation. The positive-going band centered at 2168 cm^{-1} can still be observed, confirming that this feature belongs to species in the solution rather than an adsorbed reaction intermediate. The observation of the 2168 cm^{-1} band in the ATR-IR spectrum of 0.1 M KCNO + 1 M KOH solution, referenced to 1 M KOH, confirmed that this feature is related to NCO$^-$. The formation of cyanate ion indicates a partial oxidation of urea in which only one C–N bond was cleaved. For Ni/C, the increase of NCO$^-$ became more progressive at potential higher than 0.6 V while the intensities of the CO_3^{2-} and HCO_3^- peaks decreased. Contrary to this, all the positive-going bands on Ni-WC/C catalyst continue to grow as the potential increases, suggesting lower adsorption energies of the intermediates. Furthermore, the CO_3^{2-} and HCO_3^- band intensities increased initially and then kept stable as the potential goes positively. Based on these spectroscopic results and electrochemical data, the authors believed that it is likely that the predominant oxidation pathway on the Ni/C electrode is the partial oxidation that leads to the production of NCO$^-$ ion and the complete

oxidation of urea to produce CO_2 becomes the predominant pathway on the Ni-WC/C surface. The much higher activity and stability of Ni-WC/C toward the UOR can be ascribed to both the easier C–N bond cleavage and anti-poisoning ability caused by the interaction between Ni and WC.

Zhang et al. [33] carried out in situ time-resolved FTIR measurements of NiClO-D (NiClOH nanosheets after electrochemical oxidation) and NiOH-D (Ni(OH)$_2$ nanosheets after electrochemical oxidation) catalysts at UOR conditions. Both of the NiClO-D and NiOH-D catalysts exhibit a vibration peak at 2168 cm^{-1} attributed to CNO$^-$ intermediate that becomes stronger as the potential increases. The vibration peak of CNO$^-$ intermediate becomes much more pronounced for NiClO-D catalyst than that of NiOH-D as the measurement time increases. Such an observation reflects that the NiClO-D catalyst has faster reaction kinetics than NiOH-D catalyst. Besides, strong C=O vibration peaks (1720 cm^{-1}) were observed in the spectra of the NiOH-D catalyst, while no obvious accumulations of C=O intermediates were found for the NiClO-D catalyst. This difference can be explained by the lattice oxygen-involved reaction pathway for NiClO-D catalyst proposed by the authors, and C=O intermediate is more facilely converted to COO* intermediate and then CO_2 gas. Notably, the spectra of NiClO-D catalyst indeed featured CO_2 vibration peaks located at 2390 cm^{-1} while no sign of CO_2 vibration peaks was found for NiOH-D catalyst. Based on the fact that the generated CO_2 gas is easy to react with KOH aqueous electrolyte, these results indicate much more amount of CO_2 gas generated from NiClO-D under the same experimental condition, suggesting the faster reaction kinetics of NiClO-D catalyst. Another difference is that the spectra of NiOH-D catalyst featured a vibration peak at 1635 cm^{-1}, which is assigned to N–H vibration in amide (–CONNH) groups. In contrast, no sign of such peak was found for NiClO-D catalyst. These results provide spectroscopic evidence for the two different reaction pathways for NiClO-D and NiOH-D catalysts, combined with DFT simulation that the step of forming –CONNH group in the conventional pathway is replaced by the lattice-oxygen-involved COO* formation step in the new pathway. The faster kinetics for CNO$^-$ formation and adsorbed *COO desorption of NiClO-D catalyst correlate well with its enhanced catalytic performance.

Thus, it can be realized that in situ FTIR can characterize some urea oxidation products, such as CO_2

and cyanate ion, which plays an important role in the study of urea dissociation reaction paths.

Table 1. Summary of the in situ characterization techniques for Ni-based UOR electrocatalysts.

Technique	Function	Probing region	Detection species
Raman	surface species	interface	bending and stretching vibrations indicating the transformation from $Ni(OH)_2$ to NiOOH; symmetric stretch of CO_3^{2-}
XRD	crystal structure	solid	diffraction peak (~12.7°) indexed to NiOOH (003) reflection
FTIR	chemisorbed species on catalyst	interface	OH^- concentration change near the electrode during the formation of NiOOH; cleavage of C–N bonds; formation of CO_3^{2-}, HCO_3^- and intermediate CNO^-

3. SUMMARY AND OUTLOOK

In situ spectroscopic techniques can provide mechanistic information regarding catalyst dynamics, reaction intermediate identity and more. In situ Raman spectroscopy and in situ XRD can obtain information about the structural and electronic state changes of the heterojunction between the catalyst electrode and electrolyte under real electrochemical reaction conditions, revealing the true active sites or active species of electrocatalysts during use. In situ IR spectroscopy is very powerful in the detection of reaction intermediate and key products, and plays a significant role in the study of reaction paths. A brief overview of the contribution of each technique is summarized in Table 1. Although the research on Ni-based multi-component electrocatalysts for UOR is progressing rapidly, in situ study on their actual working conditions is scarce. The existing reports of using in situ Raman to characterize bimetallic electrocatalysts have not clearly obtained the information of doped metal elements, thus more research is needed to better reveal the role of multi-components such as doped metal elements and the corresponding reaction mechanism. The ongoing work of our group has obtained in situ

characterization results of typical bimetallic component catalysts, and recognized the important role of high-valence species including the second metal element other than Ni during the UOR. In addition, since each technique has strengths and limitations, the integrated utilization of multiple in situ techniques is also highly desired.

REFERENCE

[1] Munoz LAH, Huijben JCCM, Verhees B, Verbong GPJ. The power of grid parity: A discursive approach. Technol Forecast Soc Change 2014;87:179-90.

[2] Fu J, Cano ZP, Park MG, Yu AP, Fowler M, Chen ZW. Electrically rechargeable zinc-air batteries: Progress, challenges, and perspectives. Adv Mater 2017;29:1604685.

[3] Rollinson AN, Jones J, Dupont V, Twigg MV. Urea as a hydrogen carrier: A perspective on its potential for safe, sustainable and long-term energy supply. Energ Environ Sci 2011;4:1216-24.

[4] Lan R, Irvine JTS, Tao SW. Ammonia and related chemicals as potential indirect hydrogen storage materials. Int J Hydrogen Energy 2012;37:1482-94.

[5] Xu W, Wu Z, Tao S. Urea-based fuel cells and electrocatalysts for urea oxidation. Energy Technol 2016;4:1329-37.

[6] Boggs BK, King RL, Botte GG. Urea electrolysis: Direct hydrogen production from urine. Chem Commun 2009;4859-61.

[7] Lan R, Tao S, Irvine JTS. A direct urea fuel cell - power from fertiliser and waste. Energ Environ Sci 2010;3:438-41.

[8] Yu BB, Zhang HM, Xu W, Li G, Wu ZC. Remediation of chromium-slag leakage with electricity cogeneration via a urea-Cr(VI) cell. Sci Rep-Uk 2014;4:5860.

[9] Xu W, Zhang HM, Li G, Wu ZC. A urine/Cr(VI) fuel cell - Electrical power from processing heavy metal and human urine. J Electroanal Chem 2016;764:38-44.

[10] Zhang HM, Wang YF, Wu ZC, Leung DYC. A direct urea microfluidic fuel cell with flow-through Ni-supported-carbon-nanotube-coated sponge as porous electrode. J Power Sources 2017;363:61-9.

[11] Zhu BJ, Liang ZB, Zou RQ. Designing advanced catalysts for energy conversion based on urea oxidation reaction. Small 2020;16:1906133.

[12] Sun XJ, Ding R. Recent progress with electrocatalysts for urea electrolysis in alkaline media

for energy-saving hydrogen production. Catal Sci Technol 2020;10:1567-81.

[13] Xu W, Du DW, Lan R, Humphreys J, Wu ZC, Tao SW. Highly active Ni-Fe double hydroxides as anode catalysts for electrooxidation of urea. New J Chem 2017;41:4190-6.

[14] Miao YQ, Ouyang L, Zhou SL, Xu L, Yang ZY, Xiao MS, Ouyang RZ. Electrocatalysis and electroanalysis of nickel, its oxides, hydroxides and oxyhydroxides toward small molecules. Biosens Bioelectron 2014;53:428-39.

[15] Xu W, Du DW, Lan R, Humphreys J, Miller DN, Walker M, Wu ZC, Irvin JTS, Tao SW. Electrodeposited NiCu bimetal on carbon paper as stable non-noble anode for efficient electrooxidation of ammonia. Appl Catal B-Environ 2018;237:1101-9.

[16] Vedharathinam V, Botte GG. Understanding the electro-catalytic oxidation mechanism of urea on nickel electrodes in alkaline medium. Electrochim Acta 2012;81:292-300.

[17] Xu W, Zhang HM, Li G, Wu ZC. Nickel-cobalt bimetallic anode catalysts for direct urea fuel cell. Sci Rep-Uk 2014;4:5863.

[18] Yang X, Xu W, Zhang H, Wu Z. $Ni_xCo_{3-x}O_4$ nanowire arrays grown on carbon fiber cloth as efficient electrocatalysts for urea oxidation. Energy Procedia 2017;142:1414-20.

[19] Yan W, Wang D, Botte GG. Electrochemical decomposition of urea with Ni-based catalysts. Appl Catal B-Environ 2012;127:221-6.

[20] Yan W, Wang D, Botte GG. Template-assisted synthesis of Ni-Co bimetallic nanowires for urea electrocatalytic oxidation. J Appl Electrochem 2015;45:1217-22.

[21] Guo F, Ye K, Cheng K, Wang G, Cao D. Preparation of nickel nanowire arrays electrode for urea electro-oxidation in alkaline medium. J Power Sources 2015;278:562-8.

[22] Yang D, Yang L, Zhong L, Yu X, Feng L. Urea electro-oxidation efficiently catalyzed by nickel-molybdenum oxide nanorods. Electrochim Acta 2019;295:524-31.

[23] Guo F, Ye K, Du M, Huang X, Cheng K, Wang G, Cao D. Electrochemical impedance analysis of urea electro-oxidation mechanism on nickel catalyst in alkaline medium. Electrochim Acta 2016;210:474-82.

[24] Deng YL, Handoko AD, Du YH, Xi SB, Yeo BS. In situ raman spectroscopy of copper and copper oxide surfaces during electrochemical oxygen evolution reaction: Identification of Cu^{III} oxides as catalytically active species. ACS Catal 2016;6:2473-81.

[25] Deng YL, Yeo BS. Characterization of electrocatalytic water splitting and CO_2 reduction reactions using in situ/operando raman spectroscopy. ACS Catal 2017;7:7873-89.

[26] Vedharathinam V, Botte GG. Direct evidence of the mechanism for the electro-oxidation of urea on $Ni(OH)_2$ catalyst in alkaline medium. Electrochim Acta 2013;108:660-5.

[27] Vedharathinam V, Botte GG. Experimental investigation of potential oscillations during the electrocatalytic oxidation of urea on Ni catalyst in alkaline medium. J Phys Chem C 2014;118:21806-12.

[28] Singh RK, Subramanian P, Schechter A. Enhanced urea activity of oxidation on nickel-deposited tin dendrites. Chemelectrochem 2017;4:1037-43.

[29] Zhang K, Zhang G, Qu J, Liu H. Intensification of anodic charge transfer by contaminant degradation for efficient H_2 production. J Mater Chem A 2018;6:10297-303.

[30] Wang D, Botte GG. In situ X-ray diffraction study of urea electrolysis on nickel catalysts. Ecs Electrochemistry Letters 2014;3:H29-H32.

[31] Mahoney EG, Sheng WC, Cheng M, Lee KX, Yan YS, Chen JGG. Analyzing the electrooxidation of ethylene glycol and glucose over platinum-modified gold electrocatalysts in alkaline electrolyte using in-situ infrared spectroscopy. J Power Sources 2016;305:89-96.

[32] Wang L, Zhu SQ, Marinkovic N, Kattel S, Shao MH, Yang BL, Chen JGG. Insight into the synergistic effect between nickel and tungsten carbide for catalyzing urea electrooxidation in alkaline electrolyte. Appl Catal B-Environ 2018;232:365-70.

[33] Zhang LS, Wang LP, Lin HP, Liu YX, Ye JY, Wen YZ, Chen A, Wang L, Ni FL, Zhou ZY, Sun SG, Li YY, Zhang B, Peng HS. A lattice-oxygen-involved reaction pathway to boost urea oxidation. Angew Chem Int Edit 2019;58:16820-5.